Protonation and Subsequent Intramolecular Hydrogen Bonding as a Method to Control Chain Structure and Tune Luminescence in Heteroatomic Conjugated Polymers

ARTICLE *in* JOURNAL OF THE AMERICAN CHEMICAL SOCIETY · JUNE 2002

Impact Factor: 12.11 · DOI: 10.1021/ja012409+ · Source: PubMed

7 AUTHORS, INCLUDING:

Andy Monkman
Durham University
416 PUBLICATIONS **9,794** CITATIONS
SEE PROFILE

Lars-Olof Palsson Dr
Durham University
71 PUBLICATIONS **1,944** CITATIONS
SEE PROFILE

J|A|C|S
ARTICLES
Published on Web 05/03/2002

Protonation and Subsequent Intramolecular Hydrogen Bonding as a Method to Control Chain Structure and Tune Luminescence in Heteroatomic Conjugated Polymers

Andrew P. Monkman,*,† Lars-Olof Pålsson,† Roger W. T. Higgins,† Changsheng Wang,‡ Martin R. Bryce,*,‡ Andrei S. Batsanov,‡ and Judith A. K. Howard‡

Contribution from the Department of Physics and the Department of Chemistry, University of Durham, South Road, Durham DH1 3LE, United Kingdom

Received October 22, 2001

Abstract: We report the effects of protonation on the structural and spectroscopic properties of 1,4-dimethoxy-2,5-bis(2-pyridyl)benzene (**9**) and the related AB copolymer poly{2,5-pyridylene-*co*-1,4-[2,5-bis(2-ethylhexyloxy)]phenylene} (**7**). X-ray crystallographic analysis of **9**, 1,4-dimethoxy-2,5-bis(2-pyridyl)-benzene bis(formic acid) complex **10**, and 1,4-dimethoxy-2,5-bis(2-pyridinium)benzene bis(tetrafluoroborate salt) (**11**) establishes that reaction of formic acid with **9** does not form an ionic pyridinium salt in the solid state, rather, the product **10** is a molecular complex with strong hydrogen bonds between each nitrogen atom and the hydroxyl hydrogen in formic acid. In contrast, reaction of **9** with tetrafluoroboric acid leads to the dication salt **11** with significant intramolecular hydrogen bonding (N−H···O−Me) causing planarization of the molecule. The pyridinium and benzene rings in **11** form a dihedral angle of only 3.9° (cf. pyridine−benzene dihedral angles of 35.4° and 31.4° in **9**, and 43.8° in **10**). Accordingly, there are large red shifts in the optical absorption and emission spectra of **11**, compared to **9** and **10**. Polymer **7** displays a similar red shift in its absorption and photoluminescence spectra upon treatment with strong acids in neutral solution (e.g. methanesulfonic acid, camphorsulfonic acid, and hydrochloric acid). This is also observed in films of polymer **7** doped with strong acids. Excitation profiles show that emission arises from both protonated and nonprotonated sites in the polymer backbone. The protonation of the pyridine rings in polymer **7**, accompanied by intramolecular hydrogen bonding to the oxygen of the adjacent solubilizing alkoxy substituent, provides a novel mechanism for driving the polymer into a near-planar conformation, thereby extending the π-conjugation, and tuning the absorption and emission profiles. The electroluminescence of a device of configuration ITO/PEDOT/polymer **7**/Ca/Al is similarly red-shifted by protonation of the polymer.

Introduction

The ability to control the optical and electronic properties of luminescent conjugated oligomers or polymers is a long-held goal, which is currently an important issue in the design of new materials for organic light-emitting diodes (LEDs).[1] The great attraction of organic materials as the emissive components in large-area displays[2] stems from their low cost, the versatility of synthetic chemistry to fine-tune molecular structure and hence physical properties, and the relative ease of device fabrication. Polymers with basic nitrogen atoms offer the possibility of protonation or alkylation of the lone pair as a way of modifying their properties.[3] Recently, we have shown that polymers containing pyridine repeat units are of considerable interest in the areas of electron transport[4] and new tailored luminescent materials.[5] It is important to investigate the role of protonation in this class of polymers because poly(2,5-pyridylene) (PPY) and some copolymers are soluble only in acids such as formic, dichloroacetic, and sulfuric[6] and the acidic alcohol, hexafluoro-2-propanol.[7] Formic acid is the most frequently used solvent for PPY as it facilitates easy spinning of high-quality thin films for device applications. Thus an important issue is whether formic acid is retained in the thin films after spinning, and if

* Corresponding authors. E-mail: a.p.monkman@durham.ac.uk; m.r.bryce@durham.ac.uk.
† Department of Physics.
‡ Department of Chemistry.

(1) Reviews: (a) Kraft, A.; Grimsdale, A. C.; Holmes, A. B. *Angew. Chem., Int. Ed. Engl.* **1998**, *37*, 402. (b) Segura, J. L. *Acta Polym.* **1998**, *49*, 319. (c) Mitschke, U.; Bäuerle, P. *J. Mater. Chem.* **2000**, *10*, 1471. (d) Segura, J. L.; Martín, N. *J. Mater. Chem.* **2000**, *10*, 2403.
(2) (a) Gustafsson, G.; Cao, Y.; Treacy, G. M.; Klavetter, F.; Colaneri, N.; Heeger, A. J. *Adv. Mater.* **1992**, *357*, 477. (b) Gu, G.; Burrows, P. E.; Venkatesh, S.; Forrest, S. R.; Thompson, M. E. *Opt. Lett.* **1997**, *22*, 172. (c) Friend, R. H.; Gymer, R. W.; Holmes, A. B.; Burroughes, J. H.; Marks, R. N.; Taliani, C.; Bradley, D. D. C.; dos Santos, D. A.; Brédas, J. L.; Logdlund, M.; Salaneck, W. R. *Nature* **1999**, *397*, 121. (d) Visser, R. J. *Philips J. Res.* **1998**, *51*, 467. (e) See the webpage of CDT: http://www.cdtltd.co.uk.
(3) Wang, H.; Helgeson, R.; Bin, M.; Wudl, F. *J. Org. Chem.* **2000**, *65*, 5862.
(4) Dailey, S.; Halim, M.; Rebourt, E.; Samuel, I. D. W.; Monkman, A. P. *J. Condens. Matter* **1998**, *10*, 5171.
(5) Wang, C.; Kilitziraki, M.; McBride, J. A. H.; Bryce, M. R.; Horsburgh, L. E.; Sheridan, A. K.; Monkman, A. P.; Samuel, I. D. W. *Adv. Mater.* **2000**, *12*, 217.
(6) Yamamoto, T.; Murauyama, T.; Zhou, Z.-h.; Ito, T.; Fukuda, T.; Yoneda, Y.; Begum, F.; Ikeda, T.; Sasaki, S.; Takezoe, H.; Fukuda, A.; Kubota, K. *J. Am. Chem. Soc.* **1994**, *116*, 4832.
(7) Yamamoto, T.; Choi, B. K.; Takeuchi, M.; Kubota, K. *Chem. Lett.* **1999**, *10*, 1049.

Chart 1. 1,4-Phenylene-2,5-pyridylene Copolymers **1** and **2**[5]

1 **2**

so, to what degree is the polymer protonated in the solid state. Formic acid is not present in thin PPY films at concentrations measurable by X-ray photoelectron spectroscopy (XPS), but the addition of less volatile acids such as camphorsulfonic acid (CSA) to the PPY formic acid solutions allowed protonated PPY films to be cast.[8] In these films changes occurred to both absorption and emission properties of the PPY, and it was possible to produce films with pseudo white light emission which retained very respectable photoluminescence quantum yields (PLQY).[8]

In the search for new electron transporting polymers 1,4-phenylene-2,5-pyridylene copolymers **1** and **2** (Chart 1) were studied.[5] In contrast to other pyridine-containing polymers,[6,9] polymers **1** and **2** were synthesized by Suzuki coupling[10] to achieve a regular AB structure. The solubility of polymers **1** and **2** in solvents ranging from neutral, e.g., chloroform, to acidic, e.g., formic acid, allowed the effects of protonation to be studied. A significant red shift was seen in the absorption spectrum of polymer **1** in acidic solvents, but not for polymer **2**.[5] To explore this feature in detail we have now synthesized the phenylene−pyridylene copolymer **7** and the model teraryl compound **9**. Their structural and photophysical properties before and after protonation have been studied. In particular, we now demonstrate that protonation of the pyridyl nitrogen has an important structural effect: intramolecular hydrogen bonding to the adjacent oxygen atom in the alkoxy substituent planarizes the backbone of the molecules, which leads to red shifts of both the optical absorption and emisson spectra. By using different acids in combination with polymer **7** to control this protonation/intramolecular hydrogen bonding process we can tune the emission spectra in the solid state by ca. 0.5 eV. This mechanism is distinctly different from that reported during the course of this work by Meijer et al.[11] in which hydrogen bonding in a *neutral* oligomer/copolymer facilitates coplanarity of the adjacent aryl/heteroaryl units.

Results and Discussion

Synthesis. The synthesis of polymer **7** is shown in Scheme 1. Solubilizing 2-ethylhexyloxy chains were added to dibromohydroquinone **3** to afford **4**[12] in 74% yield. Conversion to the diboronic acid **5** proceeded in 38% yield under standard conditions. Suzuki-type polymerization[10] of an equimolar mixture of **5** and 2,5-dibromopyridine **6** in tetrahydrofuran solutions afforded copolymer **7** as a yellow solid in high yield, with good solubility in a range of organic solvents. Gel permeation chromatography indicated $M_w = 12\,000$, $M_n = 7\,400$, and a polydispersity of 2.46 (in THF solution with polystyrene standard).

Scheme 1[a]

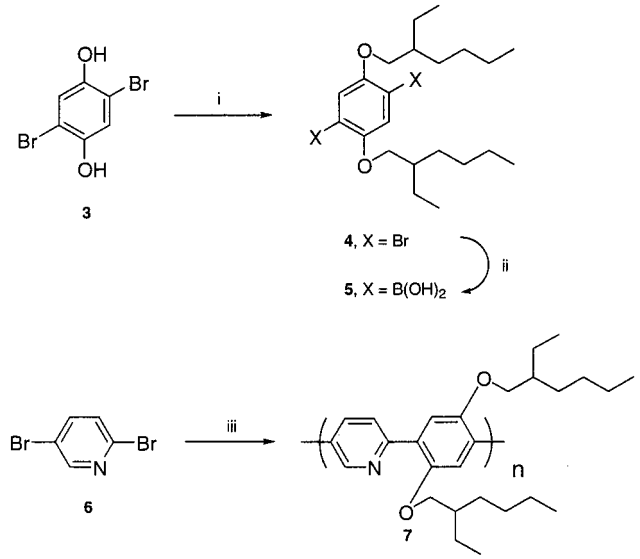

[a] Key: (i) 2-ethylhexyl bromide, DMF, K_2CO_3, 100 °C. (ii) Dry THF, BuLi then triisopropyl borate, followed by H_2O and HCl. (iii) Compound **5**, THF, $Pd(PPh_3)_4$, Na_2CO_3, Reflux.

The model compound **9** was similarly obtained in 89% yield from the diboronic acid **8**[5] and 2-bromopyridine (Scheme 2). Dissolution of **9** in ethyl acetate followed by addition of formic acid and evaporation of the solution gave the di(formic acid) complex **10** as the only product. The bis(tetrafluoroborate) salt **11** was obtained by adding fluoroboric acid in ether to a solution of **9** in methanol.

Absorption and Emission Spectroscopy. The solid-state absorption and emission spectra of polymer **7** as a function of protonation level are shown in Figures 1 and 2, respectively, which depict the general spectroscopic behavior of this class of AB polymers upon protonation of thin films. In the neutral state the lowest energy absorption maxima is observed at 3.25 eV. On protonation with methanesulfonic acid (MSA) this band red shifts considerably reaching a minimum of 2.8 eV. The shift depends to some degree on the strength of the acid used. A weak second absorption at 4.1 eV in the neutral polymer also red shifts to 3.85 eV. Whereas the low-energy feature decreases in relative oscillator strength upon protonation, the higher energy feature increases. Previous theoretical calculations[13] have shown that the $^1(\pi-\pi^*)$ transition is of lower energy than the $^1(n-\pi^*)$ transition in PPY, thus we ascribe the lowest energy transition observed in **7** to the $^1(\pi-\pi^*)$ transition. As the higher energy feature also red shifts and increases in oscillator strength on protonation we also ascribe it to a $^1(\pi-\pi^*)$ transition, as an

(8) Monkman, A. P.; Halim, M.; Samuel, I. D. W.; Horsburgh, L. *J. Chem. Phys.* **1998**, *109*, 10372.
(9) (a) Epstein, A. J.; Blatchford, J. W.; Wang, Y. Z.; Jessen, S. W.; Gebler, D. D.; Lin, L. B.; Gustafson, T. L.; Wang, H.-L.; Park, Y. W.; Swager, T. M.; MacDiarmid, A. G. *Synth. Met.* **1996**, *78*, 253. (b) Yamamoto, T.; Sugiyama, K.; Kushida, T.; Inoue, T.; Kanbara, T. *J. Am. Chem. Soc.* **1996**, *118*, 3930. (c) Marsella, M.; Fu, D.-K.; Swager, T. M. *Adv. Mater.* **1995**, *7*, 145. (d) Tian, J.; Wu, C.-C.; Thompson, M. E.; Sturm, J. C.; Register, R. A.; Marsella, M. J.; Swager, T. M. *Adv. Mater.* **1995**, *7*, 395. (e) Yamamoto, T.; Zhou, Z.-h.; Kanbara, T.; Shimura, M.; Kizu, K.; Muruyama, T.; Nakamura, Y.; Fukuda, T.; Lee, B.-L.; Ooba, N.; Tomaru, S.; Kurihara, T.; Kaino, T.; Kubota, K.; Sasaki, S. *J. Am. Chem. Soc.* **1996**, *118*, 10389. (f) Epstein, A. J.; Wang, Y. Z.; Gebler, D. D.; Fu, D. K.; Swager, T. M. *Mater. Res. Soc. Symp. Proc.* **1998**, *488*, 75. (g) Kim, J. K.; Yu, J. W.; Hong, J. M.; Cho, H. N.; Kim, Y.; Kim, C. Y. *J. Mater. Chem.* **1999**, *9*, 2171. (h) Irvin, D. J.; DuBois, C. J., Jr.; Reynolds, J. R. *Chem. Commun.* **1999**, 2121. (i) Liu, Y.; Ma, H.; Jen, A. K.-Y. *J. Mater. Chem.* **2001**, *11*, 1800.
(10) Review: Schluter, A. D. *J. Polym. Sci. A: Polym. Chem.* **2001**, *39*, 1533.
(11) (a) Pieterse, K.; Vekemans, J. A. J. M.; Kooijman, H.; Spek, A. L.; Meijer, E. W. *Chem. Eur. J.* **2000**, *6*, 4597. (b) Delnoye, D. A. P.; Sijbesma, R. P.; Vekemans, J. A. J. M.; Meijer, E. W. *J. Am. Chem. Soc.* **1996**, *118*, 8717.
(12) For an alternative synthesis of **4** from **3** (34% yield) see: Irvin, J. A.; Schwendeman, I.; Lee, Y.; Abboud, K. A.; Reynolds, J. R. *J. Polym. Sci. Part A: Polym. Chem.* **2001**, *39*, 2164.
(13) Vaschetto, M. E.; Springborg, M.; Monkman, A. P. *J. Mol. Struct. (Theo. Chem.)* **1999**, *468*, 181.

Scheme 2[a]

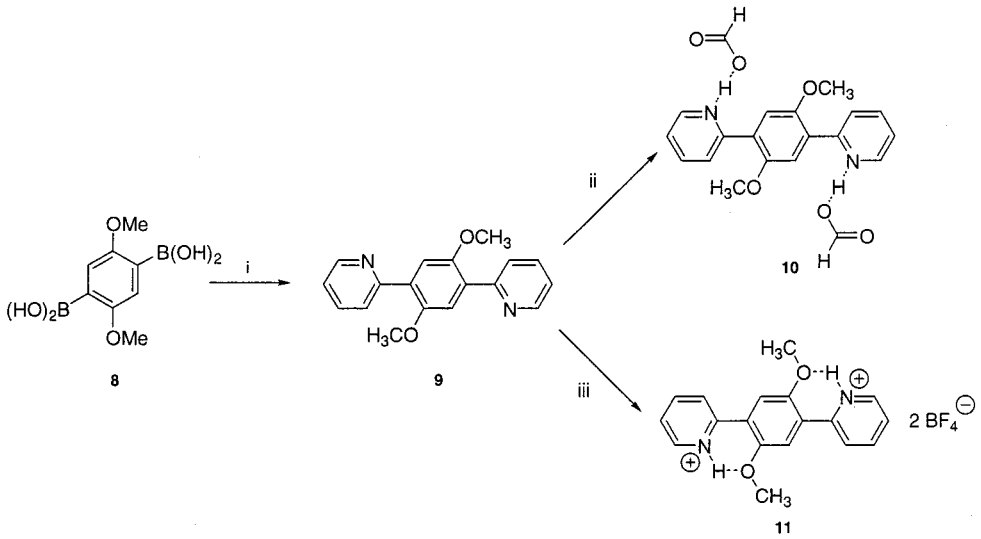

[a] Key: (i) 2-bromopyridine, THF, $Pd(PPh_3)_4$, Na_2CO_3, reflux. (ii) HCO_2H, EtOAc. (iii) HBF_4, MeOH.

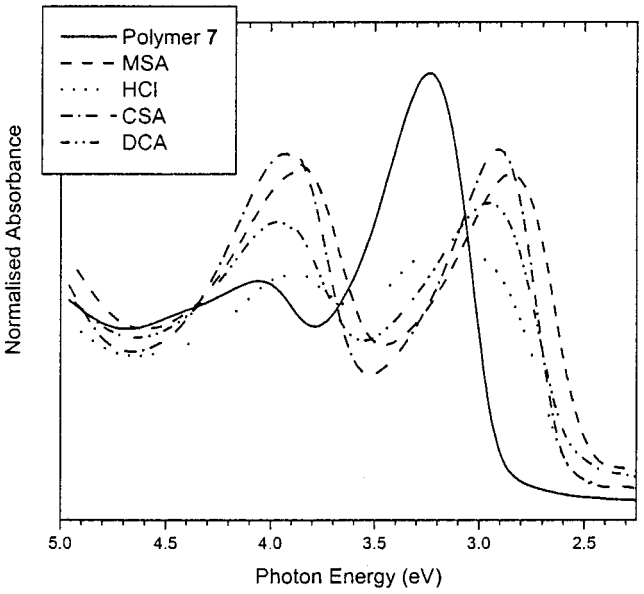

Figure 1. Absorption spectra of thin films of polymer **7** protonated with a range of acids showing that the red shift is dependent on acid strength. Abbreviations: methanesulfonic acid (MSA); camphorsulfonic acid (CSA); dichloracetic acid (DCA).

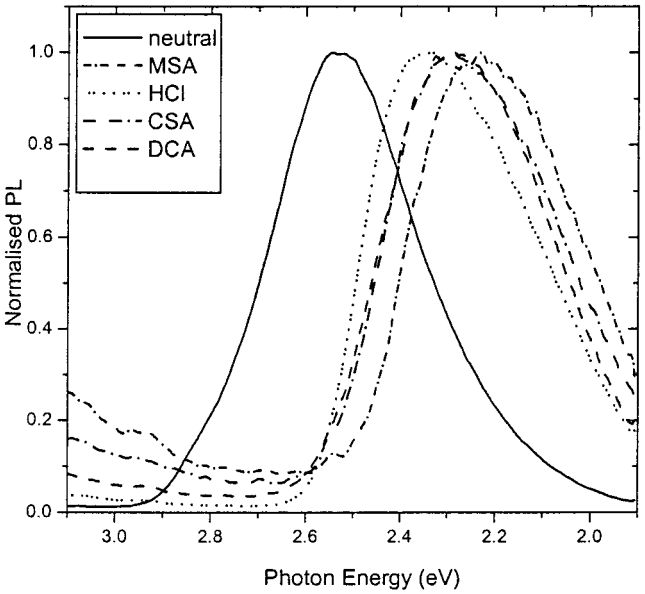

Figure 2. Normalized photoluminescence spectra of the polymer films shown in Figure 1.

(n−π*) transition should blue shift upon protonation.[13] Protonation relaxes both these states, i.e., they become more delocalized.

The red shifts observed in the absorption spectra are also mirrored in the PL spectra (Figure 2). In the case of CSA we observed that the PL band shifted from 2.55 eV to ca. 2.2 eV. The PLQY of the polymer salt films is not adversely affected by protonation with weak acids. In the case of DCA it increases from 0.20 to 0.34, whereas the stronger acids such as CSA have little effect (0.19). Only MSA causes the PLQY to drop significantly to 0.08. To determine whether the protonation process is homogeneous, excitation spectra were measured. The excitation profiles show that emission emanates from both protonated and unprotonated sites on the polymer backbone, indicating that both types of site coexist within the films. This implies that excitons do not efficiently migrate to the lowest energy sites such that luminescence from unprotonated higher energy sites is effectively quenched. These excitation profiles also show that light absorbed by the higher energy $^1(\pi-\pi^*)$ transition decays at the same energy as light absorbed by the lower energy $^1(\pi-\pi^*)$ supporting the hypothesis that the final state of these two transitions is the same, i.e., the π^* state.

Dissolution of polymer **7** in formic acid gives red shifted absorption, consistent with protonation in solution, but this shift is not observed in the spectra of thin films spun from these solutions. This is consistent with the crystallographic studies on **10** reported below. In chloroform solution, polymer **7** protonates effectively upon addition of CSA: the spectra show the same red shift as observed in the solid state. Spectra were also measured as a function of concentration in the range 10^{-3} to 10^{-6} M (in polymer repeat units). At very low concentration the absorption spectrum of the salt is very similar to that of the unprotonated polymer, although a low-energy knee is still observed on the lowest energy absorption band. This may point to an aggregation effect at high concentration. Very similar

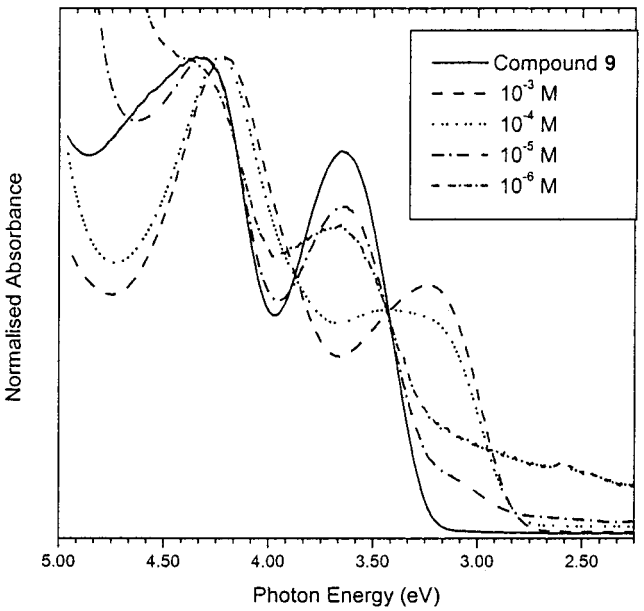

Figure 3. Absorption spectra of compound **9** protonated with CSA at various dilutions in $CHCl_3$.

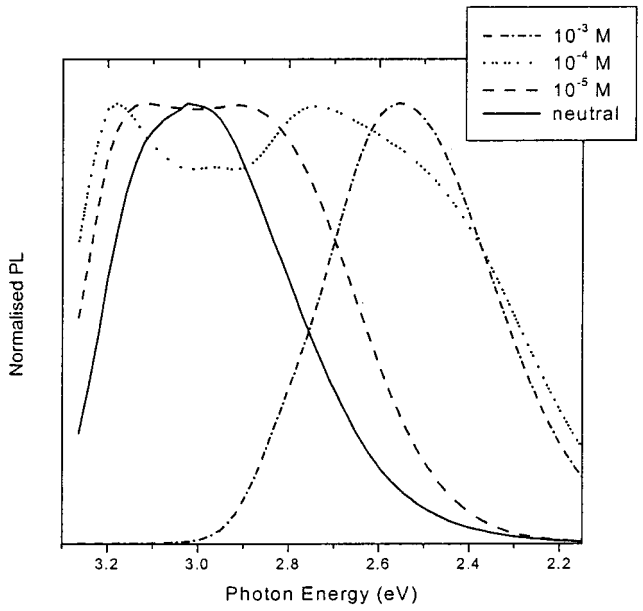

Figure 4. Normalized photoluminescence spectra of compound **9** protonated with CSA at various dilutions in $CHCl_3$.

behavior is observed for the PL in solution, with the emission showing a strong red shift at high concentrations, which is ameliorated at low concentrations. Using a stronger acid, the position becomes clearer. The absorption spectra of polymer **7** protonated with MSA remains red shifted in the presence of the acid even at 10^{-6} M. This behavior is also seen in the emission spectra of **7** protonated with MSA. As with CSA, the small degree of vibronic structure on the emission spectra of the parent polymer is lost upon protonation.

The solution spectra of polymer **7** and compound **9** are directly comparable. (Thin films of **9** could not be obtained by spin casting.) Figure 3 shows the absorption spectra of **9** with CSA as a function of concentration, which was varied by dilution of a stock (protonated) solution. Again, two absorption bands appear in the range 2.5−4.5 eV, attributed to the two lowest lying $^1(\pi-\pi^*)$ transitions; both red shift on protonation. For unprotonated **7** these bands occur at 3.6 and 4.3 eV, respectively. We also observe an isosbestic point at 3.4 eV, indicating that dilution causes a simple A → B disproportionation. Compound **9** shows very similar behavior to the polymer, as confirmed by the emission spectra (Figure 4). To investigate the homogeneity of protonation in solution, excitation spectra were measured. Figures 5 and 6 show excitation spectra for **9** protonated with CSA, monitored at 3.0 and 2.15 eV, respectively. Emission at 2.15 eV arises from absorption of light by either of the absorption bands of **9**. Observing emission at 3 eV we see that at high concentration (10^{-3} M) the protonated compound shows only a narrow band at 3.6 eV with little emission due to absorption at higher energies (Figure 5). This somewhat unusual excitation spectrum probably arises from the highly concentrated solution absorbing all the excitation light at the front surface of the cuvette; only light in the low-energy tail of the absorption band excites the whole of the solution leading to efficient collection of the emitted light. When monitoring the emission at 2.15 eV, however, it can clearly be seen that in the highly protonated state the emission comes predominantly from light absorbed at 2.8 eV, the lowest lying

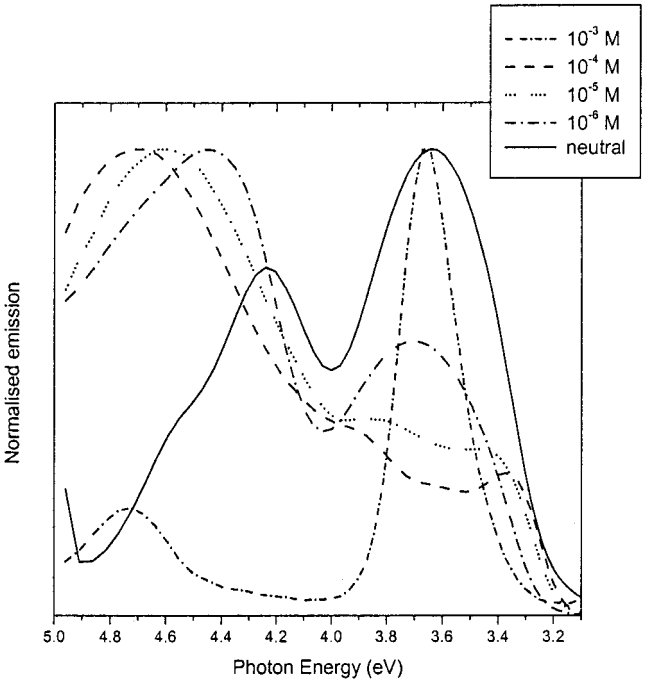

Figure 5. Excitation profiles of compound **9** protonated with CSA at various dilutions in $CHCl_3$. Emission was monitored at 3.0 eV.

absorption band in the protonated state (Figure 6). With MSA, **9** behaves in a fashion very similar to **7**.

Absorption and emission spectra of **9** were also measured in methanol solutions. We observe that with CSA methanol effectively reduces the protonation level. This is also seen with MSA, which is a stronger acid. This provides clear evidence that solvation by methanol interferes with the protonation mechanism of **9**.

To aid our understanding of the protonation mechanism with CSA, 10^{-5} M solutions of both **7** and **9**, protonated in a 1:1 ratio of CSA to pyridyl repeat unit, were prepared and their absorption spectra recorded. Excess CSA was then added to the solutions and their spectra measured again. These spectra

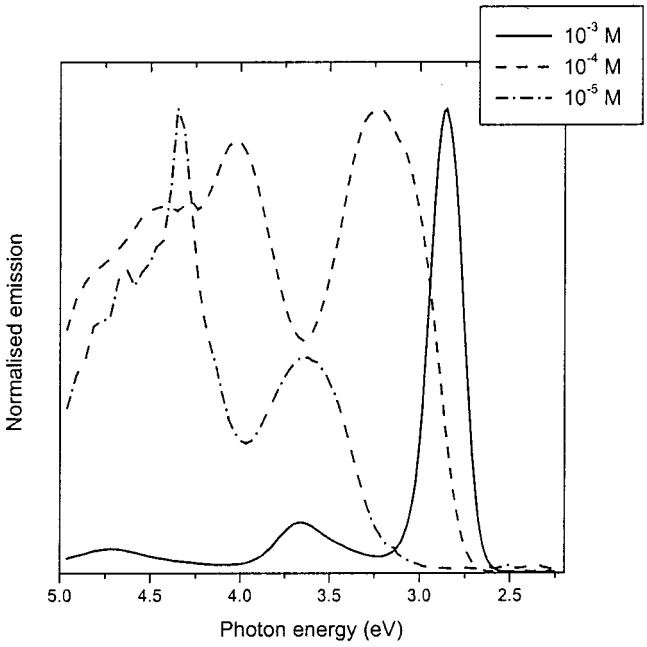

Figure 6. Excitation profiles of compound **9** protonated with CSA at various dilutions in $CHCl_3$. Emission was monitored at 2.15 eV.

are shown in the Supporting Information. In both cases the excess acid caused the full red shift of the absorption band, showing that upon dilution, the CSA equilibrium is pushed toward nondissociation and so the CSA deprotonates in the dilute regime.

The solution photophysics of both **7** and **9** establishes that energy transfer occurs from excited nonprotonated chain segments or molecules to lower energy, planar, protonated segments (molecules).[14] For **9** there is good overlap between the absorption band of the protonated molecules and the emission band of the nonprotonated molecules, suggesting that Förster energy transfer (ET) will be efficient.[15] This is further supported by the dilution studies where at low concentrations less low-energy emission is observed consistent with molecules being separated by a greater distance on average. Both polymer and molecular excitation profiles support this hypothesis where it is clearly seen that exciting anywhere in the broad absorption bands of either material gives rise to emission in the red, i.e., ET from localized twisted regions (molecules) to planar more delocalized protonated segments (molecules). In thin films of **7** this process still occurs but is not as efficient as in solution. This could be due either to a poorer spectral overlap or shorter singlet lifetime, which competes more effectively with EET.

^{1}H NMR Spectroscopy. Evidence for protonation of **9** in solution comes not only from electronic spectra but also from ^{1}H NMR data. Chart 2 shows the chemical shifts of neutral compound **9** and its diprotonated form (as the dichloride salt) in $(CD_3)_2SO$ solution. The significant downfield shifts of all the peaks from the 2-pyridyl groups, especially that of H_e which shifted by 0.56 ppm, can be explained by the protonation of the nitrogen atoms. However, the methoxy protons show a negligible shift after protonation. It is likely that the hydrogen

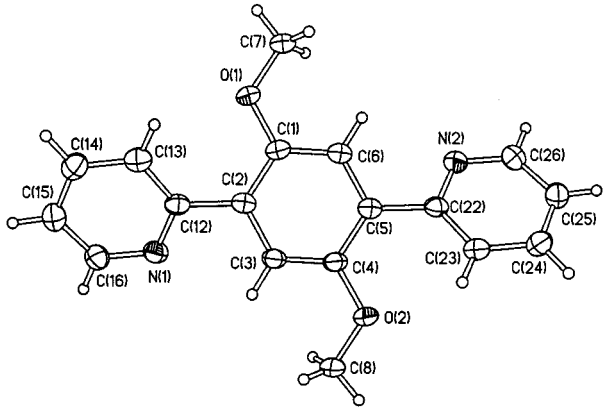

Figure 7. The ordered molecule of compound **9** in the crystal (50% displacement ellipsoids).

Chart 2. ^{1}H NMR Chemical Shifts of Compound **9** and Its Diprotonated Salt **11**, Assigned by H−H COSY and NOE Experiments

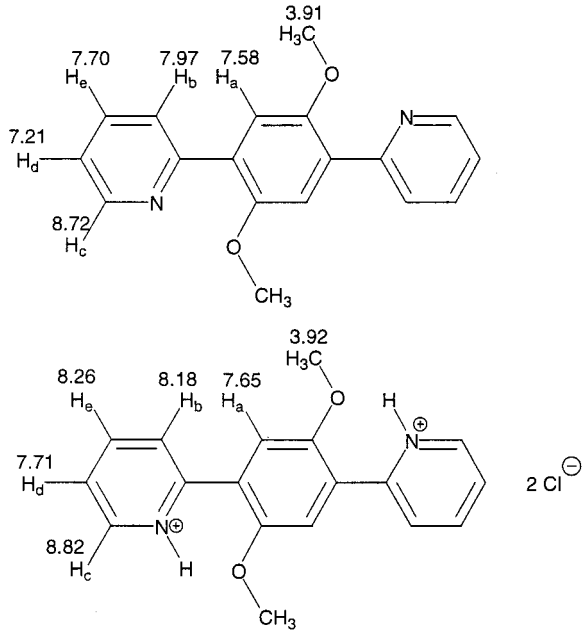

bonds observed in the solid state (Figure 9) in compound **11** are broken in DMSO solution. This competition for hydrogen bonding interactions is also evident in the UV−vis spectra of **9** with both CSA and MSA in methanol solution.

X-ray Crystal Structures of 9, 10, and 11. X-ray diffraction analysis of crystals of **9** grown from chloroform solution shows an asymmetric unit comprising two neutral molecules. One of them is ordered (Figure 7); the two pyridyl rings are not coplanar with the central benzene ring, but inclined in opposite directions, through a twist of 35.4° and 31.4° around the C(2)−C(12) and C(5)−C(22) bonds, respectively. (For PPY, a torsion angle of ca. 30° has been calculated.[13]) The pyridyl rings have mutually anti orientations of their nitrogen atoms, and each of the latter is also in an anti position relative to the adjacent methoxy group. The major conformation of the second, disordered, molecule is also twisted around the C(2)−C(12) and C(5)−C(22) bonds by 16° and 22°, respectively.

When formic acid is added to the chloroform solutions we observe that protonation occurs (see above). However, in crystals grown from ethyl acetate we isolated a molecular complex **10**

(14) (a) Jenehke, S. A.; Osaheni, J. A. *Science* **1994**, *265*, 765. (b) Grell, M.; Bradley, D. D. C.; Ungar, G.; Hill, J.; Woodhead, K. S. *Macromolecules* **1999**, *32*, 5810. (c) Nguyen, T. Q.; Doan, V.; Schartz, B. J. *J. Chem. Phys.* **1999**, *110*, 4068.
(15) Forster, T. *Discuss. Faraday Soc.* **1951**, *27*, 7.

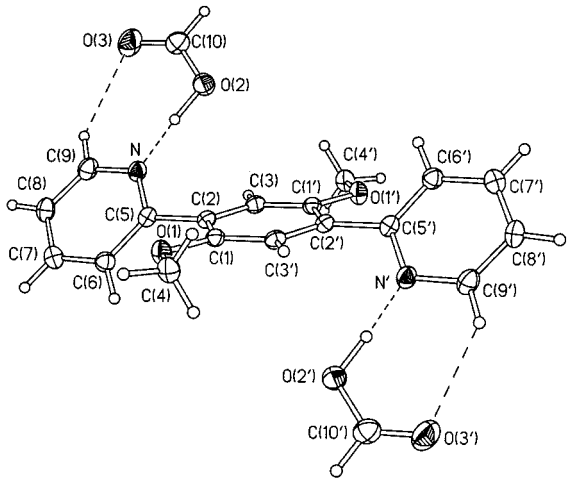

Figure 8. X-ray molecular structure of **10** (50% displacement ellipsoids). Primed atoms are generated by an inversion center. Selected distances (Å): C(10)−O(2) 1.308(2), C(10)−O(3) 1.198(2), O(2)−H(O) 1.10(3), H(O)···N 1.50(3), O(2)···N 2.593(2), H(9)···O(3) 2.50(2). Angles (deg): O(2)−H(O)−N 175(3), C(9)−H(9)−O(3) 134(2).

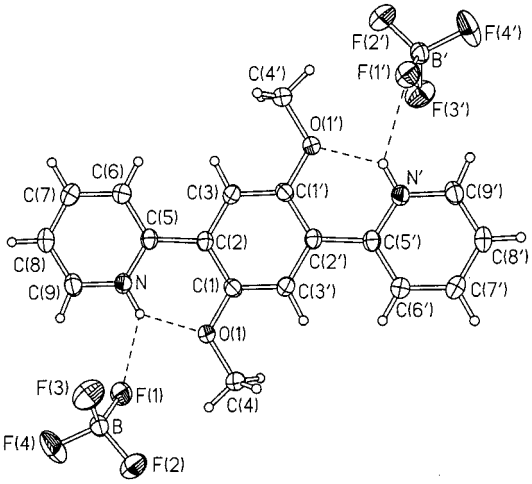

Figure 9. X-ray molecular structure of **11** (50% displacement ellipsoids). Primed atoms are generated by an inversion center. Selected distances (Å): N−H 0.90(3), H···O(1) 1.90(3), N···O(l) 2.599(2), H···F(1) 2.29 (3). Angles (deg): N−H−O(1) 132(2), N−H−F(1) 135(2).

of (neutral) **9** with two molecules of formic acid, rather than a diformate salt. The teraryl molecule in **10** is situated at a crystallographic inversion center, with two formic acid molecules linked to it by very strong hydrogen bonds (Figure 8). The hydrogen atom in the latter is located (as found in the electron density map and confirmed by successful refinement) at the O(2) atom, with no appreciable residual electron density at the N atom. The C−N−C angle of 119.5(1)° is more typical of neutral, rather than protonated, pyridine [cf. 117.8(2)° for the ordered molecule in the crystal of **9**]. The pyridine ring forms a dihedral angle of 43.8° with the benzene ring and of 15.3° with the carboxyl group.

On the contrary, with HBF_4 compound **9** is clearly diprotonated in the crystal and the product (**11**) is ionic. The dication also has crystallographic C_i symmetry. The benzene and pyridinium rings form a dihedral angle of only 3.9° and are held in this conformation by intramolecular hydrogen bonds (Figure 9). Here, the C−N−C angle is increased to 124.0(2)°, in accordance with the VSEPR theory. The dications are packed

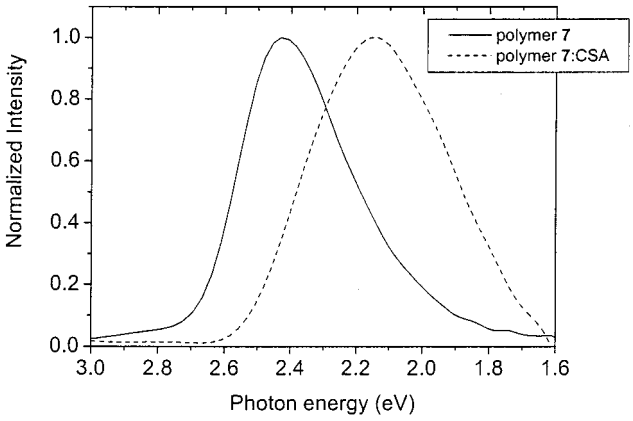

Figure 10. Electroluminescence spectra of protonated (CSA) and neutral polymer **7**.

in a dense stacking motif stabilized by electrostatic interactions with the anions, while **9** packs as dimers and **10** as looser stacks of twisted molecules.

Electroluminescence Studies. To establish if the red shift of the emission band in polymer **7** could also be observed in electroluminescence (EL) devices were made from protonated and nonprotonated polymer with a standard device configuration,[16] i.e., ITO/PEDOT/polymer **7**/Ca/Al. Thin films of **7** (100 nm thickness) were obtained by spin coating from chlorobenzene solutions with and without 1 molar equiv of CSA added to the solution. When CSA was added the spinning solution had to be diluted to enable comparable film thicknesses to be obtained due to the increased viscosity of the protonated polymer solution. The EL spectra obtained from both types of device are shown in Figure 10 and it can be seen that the electroluminescence behavior mirrors that of the PL upon protonation, with the EL peak shifting from 2.4 to 2.15 eV. Efficiency measurements reveal little difference between the neutral and protonated films; typically an efficiency of 0.02% was measured. This is very similar to values obtained for other pyridine-containing polymers[5] and is rather low due to the poor match between the ITO and HOMO levels of pyridine-containing systems.

Conclusion and Outlook

We have established a new way of tuning the emission energy of a luminescent polymer by increasing the planarity of the system by protonation of pyridine nitrogen. The steric hindrance of the required solubilizing side groups can be overcome by intramolecular hydrogen bonding, which forces the molecules into a planar configuration. This strategy is, therefore, clearly distinct from the intramolecular hydrogen bonding mechanism in *neutral* 2,5-diarylpyrazine systems studied by Meijer et al.[11] and the *inter*chain hydrogen bonding that can planarize and optically tune soluble polydiacetylenes and poly(*p*-phenylene)s.[17] As alkoxy side chains are widely used to provide solubility, our approach may be a way of producing readily soluble polymers where efficient green emission can be shifted into the longer wavelength region, which offers many challenges for displays. From photophysical measurements it has been deduced that Förster transfer is an efficient mechanism in systems **7** and

(16) Higgins, R. W. T.; Nothofer, H.-G.; Scherf, U.; Monkman, A. P. *Appl. Phys. Lett.* **2001**, *17*, 837.
(17) (a) Brown, A. J.; Rumbles, G.; Phillips, D.; Bloor, D. *Chem. Phys. Lett.* **1988**, *151*, 247. (b) Basker, C.; Lai, Y.-H.; Valiyaveettil, S. *Macromolecules* **2001**, *34*, 6255.

9 enabling excitation energy to migrate efficiently to the lowest energy, i.e. the most planar regions or molecules of the system. In molecularly doped polymer systems, this has been shown to be an effective method for the production of highly efficient saturated color devices.[18] Further studies on related heterocyclic polymers are in progress.

Acknowledgment. We thank EPSRC for funding this work.

Supporting Information Available: Description of experimental instrumentation used and synthetic details and characterization for **4**, **5**, **7**, **9**, **10**, and **11**; absorption spectra of polymer **7** protonated with CSA in the stoichiometric ratio (1:1) at 10^{-5} dilution in $CHCl_3$ and the effect on the spectrum of the addition of excess CSA; figures showing the disordered molecule of **9** in the crystal, and the crystal packing of **11** (PDF); X-ray crystallographic files (CIF). This material is available free of charge via the Internet at http://pubs.acs.org.

JA012409+

(18) Baldo, M. A.; Thompson, M. E.; Forrest, S. R. *Nature* **2000**, *403*, 750.